Sensors & Transducers, Vol. 179, Issue 9, September 2014, pp. 162-167

Sensors & Transducers

New Image Restoration Method Based on Multiple Aperture Defocus Images for Microscopic Images

[1,2] Shengli Fan, [1] Mei Yu, [1,2] Yigang Wang, [1] Gangyi Jiang
[1] Faculty of Information Science and Engineering, Ningbo University, Ningbo 315200, China
[2] Dept. of Information, Ningbo Institute of Technology Zhejiang University, Ningbo 315100, China
[1] Tel.: +86-574-87600411, fax: +86-574-87600411
[1] E-mail: yumei2@126.com

Received: 12 May 2014 /Accepted: 29 August 2014 /Published: 30 September 2014

Abstract: Image deconvolution is an effective image restoration technique to improve the quality of digital microscopic images resulting from out-of-focus blur. To solve the severely ill-posed problem of traditional Richardson–Lucy method, considering the point spread difference of various directions, a new microscope image restoration method based on multiple defocused images of different aperture is proposed. The maximum-likelihood estimation is used to suppress the ringing artifacts and noises sensitivity of microscope image. Experimental results show that the proposed algorithm performs better than Richardson–Lucy method and improve peak-signal-to-noise-rate about 4 dB. *Copyright © 2014 IFSA Publishing, S. L.*

Keywords: Digital optical microscope, Image restoration, Multiple aperture.

1. Introduction

Recently, digital optical microscope is becoming a vital tool in industry, materials science and biomedical for its intuitive, low cost and high degree of intelligence. It is hard to get a high quality focus image since the depth of field is very shallow while the optical system deviation is large. It is the primary problem that how to get a high quality focus image in digital optical microscope for follow-up observing, processing and measuring easily.

Image deconvolution is an effective image restoration technique to improve image quality. Image deconvolution can be categorized into two types, that is, blind deconvolution and non-blind deconvolution. The former is more difficult since the point spread function (PSF) is unknown. Natural image statistics together with a sophisticated variational Bayes inference algorithm are used to estimate the PSF [1], [2]. Even with a known PSF, non-blind deconvolution is still under-constrained. In our approach, we significantly reduce the artifacts in a non-blind deconvolution by taking advantage of the out-of-focus noisy image.

Image deconvolution problems are often solved by Richardson-Lucy (RL) deconvolution algorithm. Initially it was derived from Bayes's theorem in the early 1970's by Richardson and Lucy [3], [4]. The method is a nonlinear iterative method based on Bayesian analysis which computes maximum likelihood estimation adapted to poisson statistics. Two important drawbacks of RL deconvolution, however, are ringing artifacts and noises sensitivity. To suppress this problem, regularization constraints on the object are supplemented such as non-negative, total variation, and normalization, etc. [5]-[7]. Further more, some prior knowledge on the data has to be applied to stabilize the solution. By incorporating an anti-reflective boundary condition and a re-blurring step, Donatelli et al. recover a latent

image with reduced ringing with a PDE-based model [8]. Levin et al. use a sparse derivative prior to avoid ringing artifacts in deconvolution [9]. For the image deconvolution is ill-posed, the common problem that methods above must face is how to suppress ringing and noise amplification while preserving object edges.

There are motion image restoration systems that use specialized hardware, such as measurement sensors, to augment a camera to aid in the motion image restoration [10]. Other approaches are those that use multiple images as input to do the job. Rav-Acha et al. combined information in two motion blurred images [11], while Yuan et al. use information from two images, one blurry one noisy, to restore image [12]. Rav-Acha et al. present that deconvoluting use two motion-blurred images are better than one [13]. But for out-of-focus image, there are less research works. Therefore, we propose a novel defocus image restoration method based on multiple images of different aperture, which contain blur direction weight information to suppress ringing and noise amplification effect.

This paper is organized as follows: Section 2 explains imaging theory for defocus and introduces the conception of sub-PSF and sub-blur-image. In section 3 an image restoration algorithm based on multiple images of different aperture is proposed. Section 4 shows the experimental results of the method proposed by this paper and the classical Richardson-Lucy method. Finally, a conclusion is drawn.

2. Model for Defocus

Consider the standard optical theory of single lens imaging system, the object is focused when Eq.(1) is satisfied where f is focal length, u is distance of the object principal, and v is distance of the focused image from lens' plane [14], [15] as shown in Fig. 1. When an image sensor is placed at distance v', which Eq. (1) is not satisfied, all the rays from a point in the scene will land on multiple sensor points resulting in an out-of-focus blurred image.

$$\frac{1}{u}+\frac{1}{v}=\frac{1}{f}, \tag{1}$$

The relationship between the original true object image $f(x)$ and the output image $g(x)$ of the system can be represented as:

$$g(x)=h(x)*f(x)+n(x), \tag{2}$$

where * denotes the convolution operator, $h(x)$ denotes PSF of the system, and $n(x)$ is the random spatial distribution of noise.

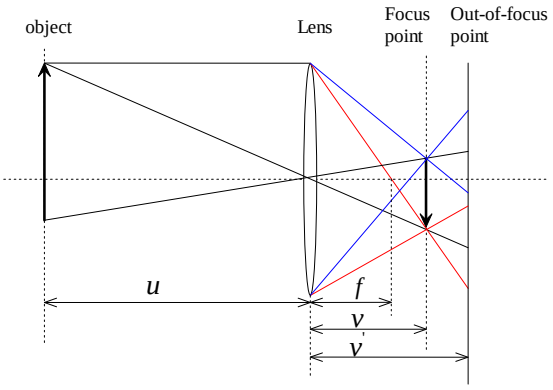

Fig. 1. Theory of image blur.

PSF depends on not only the distance of object, but also the shape and size of the lens. Usually, the lens is circular and PSF can be well approximated with a disk function. That is, a focused point will defocus as a blurred circle. Further more, the blurred circle above is composed of numbers of points which is landed by rays of different direction. To represent it, the sub-PSF $h_l(x)$ of direction *l* is introduced. PSF is decomposed into several sub-PSFs which is given by

$$h(x)=\sum_{l=1}^{n}h_l(x), \tag{3}$$

Plug Eq.(3) into Eq.(2), we got

$$g(x)=[\sum_{l=1}^{n}h_l(x)]*f(x)=\sum_{l=1}^{n}g_l(x), \tag{4}$$

where $g_l(x)$ is the sub-blurred-image which represents the diffusion amount of direction *l*.

3. Image Restoration Algorithm

There is an image restoration algorithm based on ML estimation in literature [16], [17] using the ratio of the real blurred image and estimated blurred image to calculate the deviation. Actually, blurred image is convolution of sharp image and PSF. Thus the difference is used instead of the ratio to calculate prediction deviation. Let $s^{(k)}(x)$ and $\hat{g}^{(k)}(x)$ be the estimate of $f(x)$ and $g(x)$ at iteration k, $s^{(k+1)}(x)$ be the estimate of $f(x)$ at iteration $k+1$. Then the sharp image can be obtained by iterating the following equation:

$$\Delta s^{(k)}(x)=\int_{I}h(x_i-x)\Delta g^{(k)}(x_i)dx_i, \tag{5}$$

where

$$\Delta s^{(k)}(x) = s^{(k+1)}(x) - s^{(k)}(x), \quad (6)$$

$$\Delta g^{(k)}(x) = g(x) - \hat{g}^{(k)}(x), \quad (7)$$

$$\hat{g}^{(k)}(x_i) = \int_I h(x_i - x_o) s^{(k)}(x_o) dx_o, \quad (8)$$

PSF can be well approximated with a disk function in defocus blur usually. Eq.(5) illustrates that the estimate sharp image difference $\Delta s^{(k)}(x)$ is evenly spread by the estimate blur image difference $\Delta g^{(k)}(x)$. In fact, as to the definition of sub-PSF, the diffusion of each direction is different. Thus prediction errors generated. In the iterative process, these errors will be magnified, producing ringing effects and noise amplification problems. In order to suppress above problems, the most direct and effective way is to take the direction difference into account. The difference is well characterized by the sub-blurred-images. It is expected that multiple sub-blurred-images is used instead of the original single image to get better restoration results. At applications, multiple sub-blurred-images can be obtained by changing the aperture.

Framework of the proposed image restoration method is illustrated in Fig. 2. In the iterative process, the estimated sharp image deviation $\Delta s_l^{(k)}(x)$ is computed according to each sub-PSF $h_l(x)$ and the total deviation used to update the estimated sharp image at iteration $k+1$ is the sum of above. The estimated sharp image deviation $\Delta s_l^{(k)}(x)$ has rich direction information, so the proposed image restoration method takes the spread inhomogeneity of all direction into consideration fully. The advantage of the method is that ringing effects and noise amplification problems are well solved meanwhile the effect of image restoration is guaranteed.

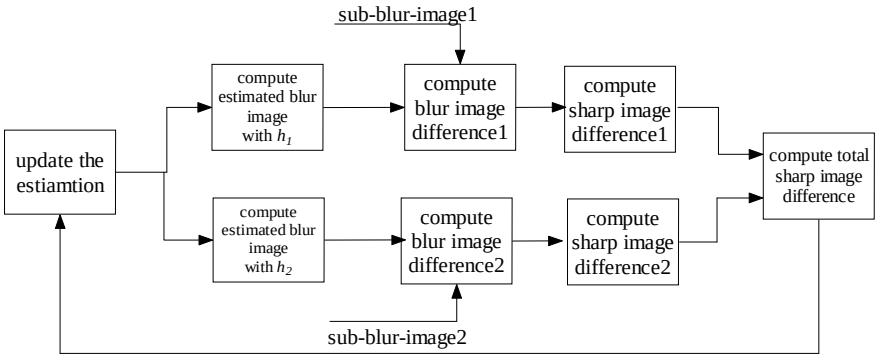

Fig. 2. Framework of multiple aperture image restoration method.

The iterative steps of algorithm are as follows:

1) Compute the estimated blur image $\hat{g}_l^{(k)}(x)$ of each direction from Eq.(8);

2) Compute the estimated blur image difference $\Delta g_l^{(k)}(x)$ from Eq.(7);

3) Compute the estimated sharp image difference $\Delta s_l^{(k)}(x)$ from Eq.(5);

4) The total estimated sharp image difference is the sum of $\Delta s_l^{(k)}(x)$;

5) Compute the total estimated sharp image $s^{(k+1)}(x)$ from Eq.(6);

6) Iteration times not reach, return to step 1), or end the iteration.

4. Experimental Result

Two sample images (512×512 pixels) including LENA image and PCB image are selected as real sharp images. LENA image is a very classic sample image with abundant band information and PCB image is a real image captured with NOVEL OPTICS NSZ-800 type optical microscope, as shown in Fig. 3(a) and Fig. 3(c). The blurred image is generated by convolving h(x) with parameters r=9, we can obtain the blurred image, as shown in Fig. 3(b) and Fig. 3(d). We applied our method to the synthetic data.

As shown in Fig. 4(a), the deviation value between estimated blurred image and the actual blurred image is not zero, which means that there are significant differences.

However, according to Eq.(5), the estimated sharp image deviation is almost zero, as shown in Fig. 4(b). These result ringing effects in deblurred image as shown in Fig. 5(a).

In order to suppress ringing effect, two sub-blur-images as shown in Fig. 4(d) and Fig. 4(e) were got by convoluting original sharp image with two different sub-PSFs h_1 and h_2, where

$$h = h_1 + h_2, \quad (9)$$

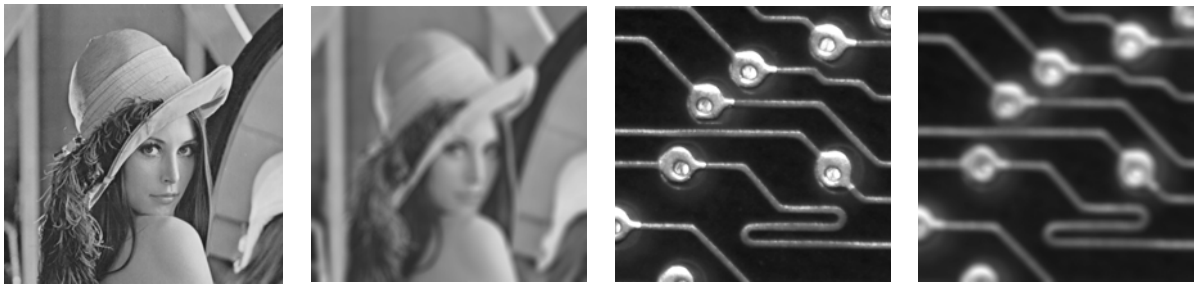

(a) (b) (c) (d)

Fig. 3. Sample image: (a) LENA sharp image; (b) LENA blur image; (c) PCB sharp image; (d) PCB blur image.

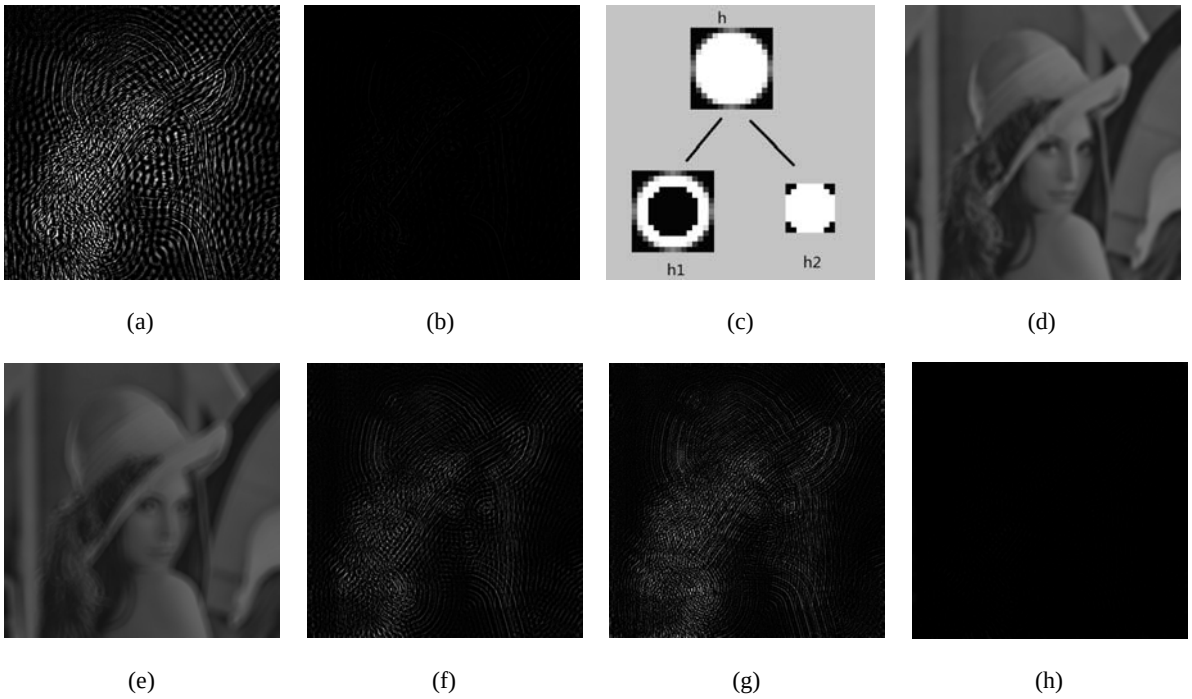

(a) (b) (c) (d)

(e) (f) (g) (h)

Fig. 4. LENA image restoration process diagram: (a) estimated blurred image deviation; (b) estimated sharp image deviation; (c) *PSF h* and sub-PSFs h_1,h_2; (d) sub-blur-image of h_1; (e) sub-blur-image of h_2; (f)estimated blurred image deviation of h_1; (g)estimated blurred image deviation of h_2; (h) estimated sharp image deviation of multiple aperture.

PSF h and sub-PSFs h_1, h_2 are shown in Fig. 4(c). Fig. 4(f), Fig. 4(g) were corresponding estimated blurred image deviation which is much smaller than Fig. 4(a). Restored image quality is greatly improved as shown in Fig. 6(b). All results are obtained in 500 iterations. In order to analyze, the pixel value of images in Fig. 4(a), Fig. 4(b), Fig. 4(f), Fig. 4(g), Fig. 4(h) is magnified 500 times.

Levin et al. use a coded aperture instead of conventional aperture to get a sharper image [9]. In our case, "coded PSF" is used instead of "disk PSF". Several sub-blur-images were got by decomposing "coded PSF" into several sub-PSFs from which a sharper image was got, as shown in Fig. 5.

Fig. 6 demonstrates the restored images of LENA by classical Richardson-Lucy method (single disk aperture image), proposed disk multiple aperture method (multiple disk aperture images), Levin's method (single coded aperture image) and proposed coded multiple aperture method (multiple coded aperture images), as shown in Fig. 6(a) ~ Fig. 6(d). While our method produces a sharper image with smaller ringing artifacts, especially in image edge area, as shown in Fig. 6(e) ~ Fig. 6(h).

(a) (b)

Fig. 5. LENA image restoration process diagram: (a) LENA blurred image by "coded PSF"; (b) coded *PSF h* and sub-PSFs h_1, h_2, h_3, h_4, h_5.

Peak Signal to Noise Ratio (PSNR) is used to evaluate the effect of image restoration. Fig. 7 and Fig. 8 demonstrate the relationship of image restore quality and iterations. In condition of same iterations, the multiple aperture image restoration method produces better result than the single aperture image restoration method. And with the increase in the iterations, the recovery results tend to stably. At this moment, the PSNR value of multiple aperture is higher than single aperture about 4 dB.

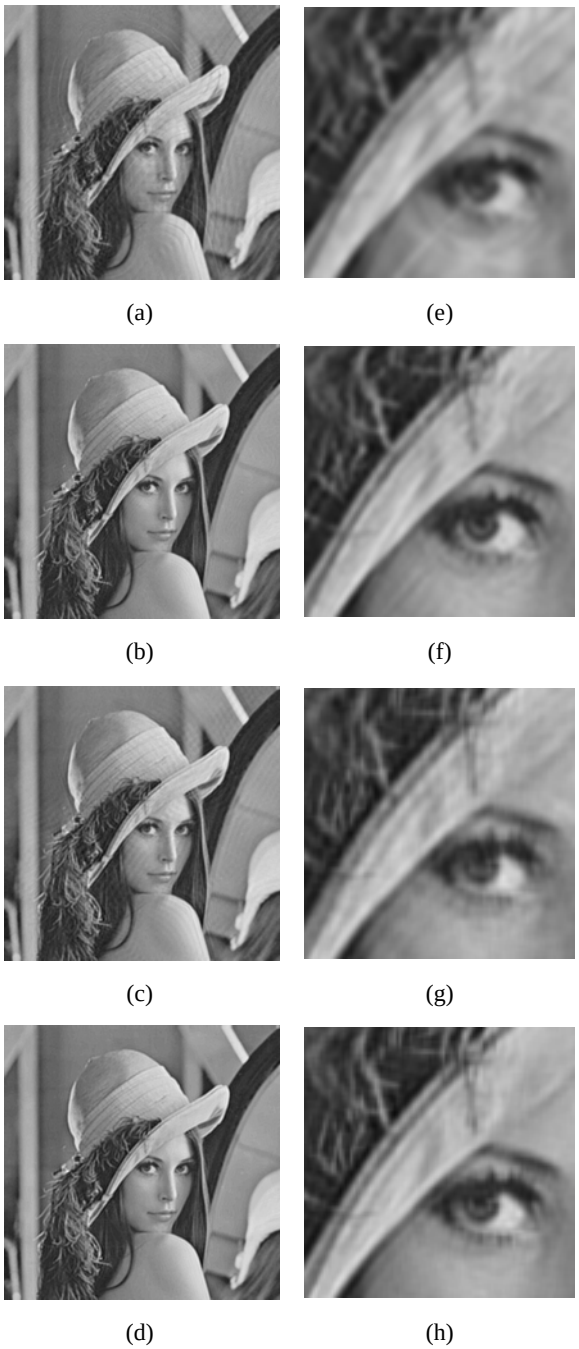

(a) (e)

(b) (f)

(c) (g)

(d) (h)

Fig. 6. Comparison of deblurring algorithms with LENA: (a) deblurred LENA image by classical Richardson-Lucy method; (b) deblurred LENA image by proposed disk multiple aperture method; (c) deblurred LENA image by Levin's method; (d) deblurred LENA image by proposed coded multiple aperture method; (e-h) details of restored images with above method.

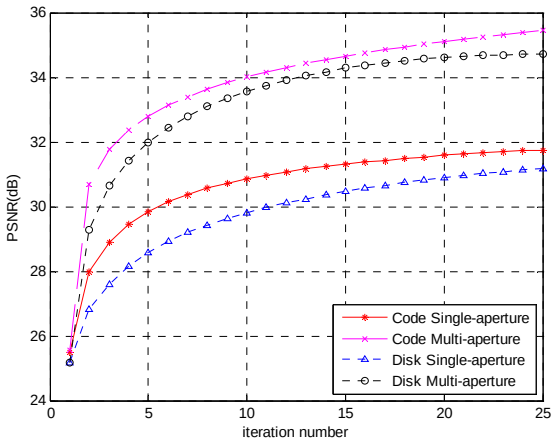

Fig. 7. Relationship of LENA image restore quality and iterations.

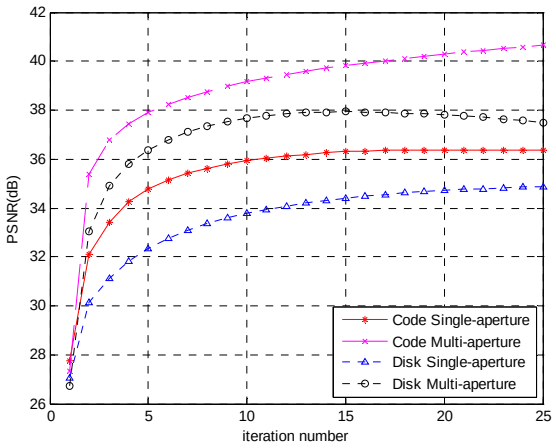

Fig. 8. Relationship of PCB image restore quality and iterations.

5. Conclusions

In this paper, an image restoration approach based on multiple images of different aperture is proposed. The cause of ringing effects and noise amplification problem is analyzed and several sub-blur-images with different direction information are used to overcome above problems. The experimental results showed that ringing effects and noise amplification problem were well suppressed and the restore quality was improved greatly. Future work may include the optimization method of combination different aperture according to different images.

Acknowledgements

This work is supported by the Natural Science Foundation of China (Grant Nos. 61271270, 61311140262).

References

[1]. R. Fergus, B. Singh, A. Hertzmann, et al, Removing camera shake from a single photograph, *ACM*

Transactions on Graphics, Vol. 26, Issue 3, 2006, pp. 787-794.
[2]. M. Ben-Ezra, S. K. Nayar, Motion-based motion deblurring, *IEEE Transactions on Pattern Analysis and Machine Intelligence*, Vol. 26, Issue 6, 2004, pp. 689-698.
[3]. L. B. Lucy, An iterative technique for the rectification of observed distributions, *Astronomical Journal*, Vol. 79, 1974, pp. 745-754.
[4]. W. H. Richardson, Bayesian-based iterative method of image restoration, *Journal of the Optical Society of America*, Vol. 62, Issue 1, 1972, pp. 55-59.
[5]. Q. Shan, L. J. Jia, A. Agarwala, High-quality motion deblurring from a single image, *ACM Transactions on Graphics*, Vol. 27, Issue 3, 2008, pp. 1-10.
[6]. D. Nicolas, B. Laure, Z. Christophe, et al, Richardson-Lucy algorithm with total variation regularization for 3D confocal microscope deconvolution, *Microscopy Research and Technique*, Vol. 69, 2006, pp. 260-266.
[7]. Y. Wang, Q. Dai, Q. Cai, et al, Blind deconvolution subject to sparse representation for fluorescence microscopy, *Optics Communications*, Vol. 286, 2013, pp. 60-68.
[8]. M. Donatelli, C. Estatico, A. Martinelli, and S. Serra-capizzano, Improved image deblurring with anti-reflective boundary conditions and re-blurring, *Inverse Problems*, Vol. 22, Issue 6, 2006, pp. 2035-2053.
[9]. A. Levin, R. Fergus, F. Durand, et al, Image and depth from a conventional camera with a coded aperture, *ACM Transactions on Graphics*, Vol. 26, Issue 3, 2007, Article No. 70, pp. 1-9.
[10]. N. Joshi, S. B. Kang, C. L. Zitnick, et al, Image deblurring using inertial measurement sensors, *ACM Transactions on Graphics*, Vol. 29, Issue 4, 2010, Article No. 30, pp. 1-9.
[11]. A. Rav-Acha, S. Peleg, Two motion-blurred images are better than one, *Pattern Recognition Letters*, Vol. 26, Issue 3, 2005, pp. 311-317.
[12]. L. Yuan, J. Sun, L. Quan, et al, Image deblurring with blurred noisy image pairs, *ACM Transactions on Graphics*, Vol. 26, Issue 3, 2007, Article No. 1.
[13]. J. Chen, C. Tang, Robust dual motion deblurring, in *Procedeengs of the IEEE Conference on Computer Vision and Pattern Recognition*, Anchorage, AK, 23-28 June 2008, pp. 1-8.
[14]. F. Paolo, B. Martin, J. Stankey, Shape from defocus via diffusion, *IEEE Transactions of Pattern Recognition and Machine Intelligence*, Vol. 30, Issue 3, 2008, pp. 518-531.
[15]. Y. Wei, C. Wu, Z. Dong, Global shape reconstruction of nano grid with singly fixed camera, *Science China – Technological Sciences*, Vol. 54, Issue 4, 2011, pp. 1044-1052.
[16]. S. Yuan, C. Preza, 3D fluorescence microscopy imaging accounting for depth-varying point-spread functions predicted by a strata interpolation method and a principal component analysis method, in *Proceedings SPIE 7904, Three-dimensional and Multidimensional Microscopy: Image Acquisition and Processing XVIII*, San Francisco, California, USA, 22 January 2011, pp. 79040M1-7.
[17]. C. Preza, J. Conchello. Depth-variant maximum-likelihood restoration for three-dimensional fluorescence microscopy, *Journal of the Optical Society of America*, Vol. 21, Issue 9, 2004, pp. 1593-1601.